Neuron, Volume *55*

Supplemental Data

Neural Dynamics of Event Segmentation in Music: Converging Evidence for Dissociable Ventral and Dorsal Networks

Devarajan Sridharan, Daniel J. Levitin, Chris H. Chafe, Jonathan Berger, and Vinod Menon

Supplemental Experimental Procedures

Behavioral study

Acquisition. A behavioral experiment was conducted to determine if transitions in the Boyce symphonies could be detected unambiguously, and to verify if there was uniformity among subjects in the perception of transitions in the stimuli. Ten subjects (non-musicians) who had previously participated in the fMRI experiment volunteered for the study. The same stimuli that were used in the scanner was used in the behavioral experiment, with the only difference that the subjects now had to respond by pushing a button whenever they heard a transition, and specifically, responded with different buttons for what they perceived to be large and small transitions. The task was programmed with E-Prime and the stimuli were presented to the subjects via noise-reducing headphones in a quiet testing area.

Data Analysis. Behavioral data from the subjects was analyzed to examine if the musically untrained subjects could unambiguously identify movement transitions. Subject responses in an observation window of t=3s before and 6s after each movement transition were analyzed to verify if the subjects were able to detect these transitions without difficulty. This window size was chosen such that there were not any marked structural changes (other than the movement transitions) occurring within this window, and there was exactly one movement transition per

observation window. Following this, three measures were constructed: (a) the number of large transitions indicated within the observation window expressed as a fraction of the total number of movement transitions viz. T_l (b) the number of transitions of any sort (large or small) indicated within the observation window expressed as a fraction of the total number of movement transitions viz. T_a, and (c) the number of large transitions indicated within the observation window expressed as a fraction of the total number of large transitions indicated by the subjects viz. T_w While the first two measures indicate how unambiguously the movement transitions are perceived, the last measure indicates how significant/important these transitions are relative to other transitions in the stimulus.

Results. The behavioral study revealed that the movement transitions could be clearly marked out by subjects even though they had had no (or very little) formal musical training. It can be seen from Figure 1 (main text), and Table S1 that subjects had a 74% success rate at correctly identifying the movement transitions as 'large' transitions (T_l=0.740) and identified more than 90% of the movement transitions as transitions of some sort (large or small, T_a=0.905). It can also be seen that the movement transitions had a high importance relative to other perceived large transitions (T_w=0.778). Furthermore, it also clear from Table S1 that the observation window was well suited to isolate responses to movement transitions alone, evidenced by T_l and T_a never exceeding unity for all subjects but one (subject #5). Hence, we consider it reasonable to assume that our subjects, even though musically untrained, had no difficulty in unambiguously perceiving the movement transitions in the scanner.

fMRI Data Acquisition

Brain images were acquired on a 3T GE Signa scanner using a standard GE whole head coil (software Lx 8.3). Images were acquired every 2 seconds in two runs that lasted 9 min 42 sec and 8 min 48 sec respectively (for a total of 18 minutes and 30 seconds). A custom-built head

holder was used to prevent head movement. 28 axial slices (4.0 mm thick, 0.5 mm skip) parallel to the AC-PC line and covering the whole brain were imaged using a T2* weighted gradient echo spiral pulse sequence (TR = 2000msec, TE = 30msec, flip angle = 70°, and 1 interleave, in-plane spatial resolution of 3.125 mm) (Glover and Lai, 1998). To reduce blurring and signal loss arising from field inhomogeneities, an automated high-order shimming method based on spiral acquisitions was used before acquiring functional MRI scans (Kim et al., 2002). Images were reconstructed by gridding interpolation and inverse Fourier transform for each time point into 64 x 64 x 28 image matrices (voxel size 3.125 x 3.125 x 4.5 mm). A linear shim correction was applied separately for each slice during reconstruction using a magnetic field map acquired automatically by the pulse sequence at the beginning of the scan (Glover and Lai, 1998). fMRI data acquisition was synchronized to stimulus presentation using a TTL pulse sent by EPRIME to the scanner timing board.

Calculation of onset latencies

Regional differences in peak latency of the BOLD response may arise from differences in either the onset or the duration of neural activity (Formisano and Goebel, 2003). In the latter case, a longer neuronal response would elicit a larger BOLD response that would take longer to reach its peak value. Onset latency of the BOLD response provides a means, in principle, of decoupling these possibilities to determine the relative onset latencies of the underlying neural activity (Formisano and Goebel, 2003; Henson et al., 2002; Menon et al., 1998). We calculated onset latencies according to the method of Sterzer and Kleinschmidt (2007). This method uses a Fourier model that can, in theory, fit any response as a linear combination of basis functions, is free of *apriori* assumptions with regard to response shape, and has been shown to be useful for characterizing the temporal aspects of the BOLD response (Sterzer and Kleinschmidt, 2007; Friston et al., 1995). The mean time-series extracted from each ROI for each subject was fitted

with a sixth order Fourier basis set (windowed with a Hanning function). Onset latencies were operationally defined as the time at which the slope of the fitted response exceeded 10% of the maximum slope of the ascending part of the response (as in Sterzer and Kleinschmidt, 2007). A paired Wilcoxon signed-rank test was then performed between regions across subjects to identify regions that differed significantly in their onset of the BOLD response (Fig. S1).

Independent Component Analysis (ICA)

Independent Component Analysis (ICA) is a model-free analysis technique that produces a set of spatially independent components and associated time courses for each subject (Beckmann and Smith, 2004). Data from the first session of the scan were preprocessed with SPM2 in a manner similar to that described in the Experimental Procedures section (in main text). The preprocessed data was then downsampled to one-half its original resolution (by sampling alternate points) in each dimension. ICA imposes heavy memory requirements on the system, and downsampling (by a factor of 2 along each dimension) was performed to reduce these requirements. ICA was then performed on the preprocessed, downsampled data using the Melodic software package (http://www.fmrib.ox.ac.uk/fsl/). Similar independent components were grouped across subjects using an in-house clustering algorithm; the algorithm computes a similarity metric using the inter-subject correlations of both the spatial map and the associated time course to create groups of similar components across subjects (Esposito et al., 2005). Components in a cluster were then masked with a gray-matter mask and entered into a second random effects analysis (Esposito et al., 2005) and height thresholded at the $p<0.001$ level, uncorrected, to create group independent component maps shown in Figure 7 (left panel). Time courses of corresponding components were averaged across subjects to produce the group time courses of the components shown in Figure 7 (right panel). GCA was performed in a manner similar to that described in the Experimental Procedures section (in main text) section

with the IC time course for each component entering the causality analysis in the place of the ROI time course used previously.

Physiological data acquisition and analysis

Acquisition. Peripheral vascular physiological data was acquired using a photoplethysmograph attached to the participant's left index finger. Pulse data was acquired as a sequence of triggers in time at the zero crossings of the pulse-waveform.

Preprocessing and artifact removal. Inter-beat intervals in the pulse data were calculated as the intervals between the triggers, these inter-beat intervals are then representative of values at the mid-point of each interval. The disadvantage with this description is that the inter-beat intervals are represented at non-uniform intervals in time. To overcome this, these intervals were then resampled to a uniform rate of 2Hz using cubic spline interpolation prior to analysis. Artifacts occur in the RR-interval data due to skipped or extra beats. Artifacts were detected by comparing the RR-interval values to the median of their predecessors and successors in a time window. Set comparison thresholds were used for elimination of unusually small (caused by extra beats) and unusually large (caused by skipped beats) intervals. Artifact removal was performed prior to interpolation and resampling. Data for each subject was further normalized to zero mean and unit variance to facilitate comparisons across subjects.

Analysis. Heart rate variability (HRV) in a time-window was calculated as the variance of the inter-beat interval within that time window (Critchley et al., 2003). A physiological observation window was defined $t=-t_1$ seconds before and $t=t_2$ second after each movement transition. HRV in the observation windows was combined (pooled) across transition events and across subjects. This was then compared to the baseline HRV (calculated from the remaining periods

outside the transition windows) across subjects and events. An F-test was used to test the difference of RR-interval variances (HRV) between the transition window and the baseline. It is to be noted that the transition could be cued by the structure in the music (such as cadences) a few seconds before the onset; hence, a broad window (t_1 + t_2) for computing variances was deemed necessary. Also, as the ANS response lag to the transition event is not well known, different values of t_1 and t_2 were used (with $t_2>t_1$) to ensure robustness of results.

Comparison to oddball paradigm of Crottaz-Herbette and Menon (2006)

Methods. Contrast images of individual subjects from the present GLM analysis and from a previous auditory oddball task (Crottaz-Herbette and Menon, 2006) were entered into a two-sample t-test to permit inferences about differential activations across the different task groups. As before, statistical parametric maps of the t-statistics were normalized to Z-scores and significant clusters of activation were determined using the joint expected probability distribution of height and extent of Z scores with height ($Z>2.33$; $p<0.01$) and extent thresholds ($p<0.05$). The resulting difference maps are shown in Figure S3 (bottom panel) and Table S4. The auditory oddball task activations alone (analyzed separately with the same height and extent thresholds) are also shown in Figure S3 (top panel) and Table S3. The movement transition activations are also shown in Figure S3 (middle panel) for comparison.

Results. Both qualitative and quantitative differences were observed between the tasks. Activations in the PTC, cingulate cortex and cerebellum overlapped with activations observed in the present study (see also Table S3). However, the PTC and extended regions of the temporo-parietal junction (TPJ) showed greater activation during movement transitions. Other areas such as the VLPFC, PPC and DLPFC, which showed strong activation during the movement transition, did not show statistically significant activation during the auditory oddball task. Thus,

the oddball task does not recruit the extensive dorsal and ventral network activations observed during passive segmentation in the present study. Further, the between-task comparison (Figure S3, bottom panel) revealed almost exactly the same set of regions that were active during the transition (Figure S3, middle panel; also see Table S4 and compare with Table S2), indicating significant quantitative differences between the oddball task activations and the dorsal-ventral stream activations observed in the present study. These findings indicate that brain processes engaged during the perception of the movement transition are distinct from those elicited by the oddball task.

Control analyses to validate onset latency and Granger causal analyses techniques

In order to further build confidence in the relatively novel mental chronometric method and Granger causal analysis (GCA) method (Figure 5B and Figure 6 in main text), we carried out the following additional control analyses.

Validation of the mental chronometric method used in the main text

(a) Converging evidence with alternate method for calculating onset latencies (Menon et al., 1998)

We calculated the onset latencies according to the method of Menon et al. (1998). The event-related BOLD response at each transition was computed for each ROI for each subject as a percentage signal change over baseline (baseline signal was computed as the mean of the signal at t= -6s, -4s and -2s relative to the transition). An event-locked average was then computed by averaging the BOLD time course across transitions and subjects. The resultant raw BOLD time courses are shown in Figure S5A (top panel) (error bars show standard error across subjects). Onset latencies of these responses were defined as the inflection point from the baseline value. Linear regression was used to fit a line to the region between 20%-70% of the peak height of the response, and the intercept of this line with the abscissa (line of zero

response) was taken as the onset point (Fig. S5A, bottom, left panel). Onset latencies were computed for the event-locked average BOLD response at each ROI for each subject separately. The mean and standard error of these onset latencies was then computed across subjects (Fig. S5A, bottom, right panel). Onset of the BOLD response in the VLPFC, in the ventral stream, preceded the DLPFC, in the dorsal stream, by about 2.39 ± 0.77 seconds (mean ± SE, p=0.0075, T_{17}=20, Wilcoxon signed rank test) and the PTC by ~1.50 ± 0.73 seconds (mean ± SE, p=0.04, T_{17}=34, Wilcoxon signed rank test) (other latency differences were not significant). Thus, we found a similar pattern of onset latency differences (as with our original method) with the earliest onsets for the VLPFC, and the VLPFC leading the DLPFC by more than 2 seconds (compare with Fig. S1 and Fig. 5B in main text). This converging pattern of results from two very different approaches (one of which uses the fitted BOLD response, and one which uses the raw BOLD response) serves to validate our findings on the early onset of the ventral regions, particularly, the VLPFC.

(b) Converging evidence with another dataset (Steinberg working memory task, Chang et al., 2007)

We applied the method of calculation of onset latencies to an alternate dataset – the Steinberg working memory task. This task requires the subjects to encode a visual stimulus during the encoding phase, maintain the stimulus during a maintenance phase and provide motor responses in the response phase (see Chang et al., 2007 for task details). We hypothesized that if our onset latency methods were reliable, we should find a difference in onsets between the visual cortex and the motor cortex. Indeed this is what we found (Fig. S5B): the visual cortex onset led motor cortex onset by 1.23s, on average, across subjects.

Methods: Visual and motor cortex ROIs were defined from task based activations (visual cortex ROI: 6mm radius sphere centered on [-36 -86 2]mm, left inferior occipital gyrus; motor cortex ROI: 6mm radius sphere centered on [-32 -3 56]mm, left precentral gyrus). Mean time series

were extracted from these ROIs across subjects, fitted with a sixth order Fourier model, and onset latencies were calculated as described above (according to the method of Sterzer and Kleinschmidt, 2007). A Wilcoxon signed rank test across subjects revealed that the visual cortex ROI onset significantly led the motor cortex ROI onset at the $p<0.05$ level.

Validation of the Granger Causal Analysis method used in the main text

Similarly, we hypothesized that we should observe causal connectivity between the visual and motor cortex, since the visual response ultimately drives the motor response (although with the caveat that we may be ignoring intermediate regions through which the connectivity may be mediated). Indeed, this is what we found: Granger causal analysis (as described in the Methods in the main text) revealed a causal link from the visual to motor cortex ROIs (defined in the previous section) across subjects (Fig. S6).

These control analyses build confidence in our onset latency and causal connectivity analysis methods, and provide support for the view that the effects observed in the present study reflect neural rather than vascular effects.

Supplemental Discussion

Passive listening task maintains ecological-validity of the listening experience

In our study, we used a passive listening task that simulates real world music listening in order to maintain ecological-validity of the listening experience. One previous study examined subject-specific brain responses to event boundaries in visual scenes wherein subjects had to indicate the occurrence of an event boundary by pressing a button inside the scanner (Zacks et al., 2001). We believe, however, that this process of active event segmentation is not part of the normal musical experience – we seldom have to make explicit decisions about where event boundaries occur while listening to music in the real-world. Such active segmentation would

also recruit decision making processes as well as extraneous motor preparation and movement related processes which are not directly relevant to event segmentation. In order to ensure that subjects were indeed able to perceive the movement transitions, we collected behavioral data in a follow-up experiment outside the scanner. This data indicated that subjects were able to detect the transitions with a high level of accuracy and consistency. Furthermore, during functional brain imaging we detected significant changes in heart rate variability at the movement transition, suggesting that these events were physiologically salient even when participants were not asked to segment the musical stream or make any explicit decisions regarding any aspect of the stimulus. While scanner tasks typically keep the subjects actively occupied so as to have them better focus on the task at hand, several previous functional imaging studies have used passive listening and/or viewing tasks similar to ours inside the scanner with considerable success (Belin et al., 2000; Hasson et al., 2004; Wilson et al., 2004).

Movement transitions are not perceived merely as pauses in the music

The complex pattern of brain responses seen during the movement transition is inconsistent with the view that these events are perceived merely as a pause occurring in the musical stream. Additional analyses conducted in our study provide further support for this view; we summarize the evidence here. First, we demonstrate that increases in amplitude levels of the stimulus modulate only the left and right auditory cortices, and do not account for the pattern of activation observed at the movement transition. Second, decreases in amplitude levels, such as those that occur at the movement transition, were not related to changes in activation in any brain region. Third, direct comparisons with an oddball task showed little overlap between responses to transitions and oddball stimuli, indicating that the movement transitions were not interpreted as sudden or unexpected oddball events. Fourth, in the follow-up behavioral experiment all subjects accurately and consistently detected virtually all of the twenty movement

transitions. Fifth, the movement transitions induced significant physiological changes that were correlated with increased brain responses in regions that are known to integrate visceral, affective and cognitive processes in response to salient stimuli (Critchley, 2005). Taken together, the evidence presented in our study suggests that movement transitions, rather than being merely interpreted as silence, are an important component of the natural music listening experience.

References (Supplemental Data)

- Belin, P., Zatorre, R.J., Lafaille, P., Ahad, P., and Pike, B. (2000). Voice-selective areas in human auditory cortex. Nature *6767,* 309-312.

- Chang, C., Crottaz-Herbette, S., and Menon, V. (2007). Temporal dynamics of basal ganglia response and connectivity during verbal working memory. Neuroimage *3,* 1253-1269.

- Critchley, H.D., Mathias, C.J., Josephs, O., O'Doherty, J., Zanini, S., Dewar, B., Cipolotti, L., Shallice, T., and Dolan, R.J. (2003). Human cingulate cortex and autonomic control: converging neuroimaging and clinical evidence. Brain *10,* 2139-2152.

- Critchley, H.D. (2005). Neural mechanisms of autonomic, affective, and cognitive integration. J. Comp. Neurol. *1,* 154-166.

- Crottaz-Herbette, S., and Menon, V. (2006). Where and when the anterior cingulate cortex modulates attentional response: Combined fMRI and ERP evidence. J. Cogn. Neurosci. *5,* 766-780.

- Esposito, F., Scarabino, T., Hyvarinen, A., Himberg, J., Formisano, E., Comani, S., Tedeschi, G., Goebel, R., Seifritz, E., and Di Salle, F. (2005). Independent component analysis of fMRI group studies by self-organizing clustering. Neuroimage *1,* 193-205.

- Formisano, E., and Goebel, R. (2003). Tracking cognitive processes with functional MRI mental chronometry. Curr. Opin. Neurobiol. *2,* 174-181.

- Glover, G.H., and Lai, S. (1998). Self-navigated spiral fMRI: interleaved versus single-shot. Magn. Reson. Med. *3,* 361-368.

- Friston, K.J., Frith, C.D., Frackowiak, R.S., and Turner, R. (1995). Characterizing dynamic brain responses with fMRI: A multivariate approach. Neuroimage *2*, 166-172.

- Henson, R.N., Price, C.J., Rugg, M.D., Turner, R., and Friston, K.J. (2002). Detecting latency differences in event-related BOLD responses: Application to words versus nonwords and initial versus repeated face presentations. Neuroimage *1,* 83-97.

- Kim, D., Adalsteinsson, E., Glover, G.H., and Spielman, D.M. (2002). Regularized higher-order in vivo shimming. Magn. Reson. Med. *4,* 715-722.

- Menon, R.S., Luknowsky, D.C., and Gati, J.S. (1998). Mental chronometry using latency-resolved functional MRI. Proc. Natl. Acad. Sci. U. S. A. *18,* 10902-10907.

- Sterzer, P., and Kleinschmidt, A. (2007). A neural basis for inference in perceptual ambiguity. Proc. Natl. Acad. Sci. U. S. A. *1,* 323-328.

- Wilson, S.M., Saygin, A.P., Sereno, M.I., and Iacoboni, M. (2004). Listening to speech activates motor areas involved in speech production. Nat. Neurosci. *7,* 701-702.

- Zacks, J.M., Speer, N.K., Swallow, K.M., Braver, T.S., and Reynolds, J.R. (2007). Event perception: a mind-brain perspective. Psychol. Bull. *2,* 273-293.

Supplemental Figures and Tables

Figure S1. Calculation of onset latencies of event-related BOLD response.

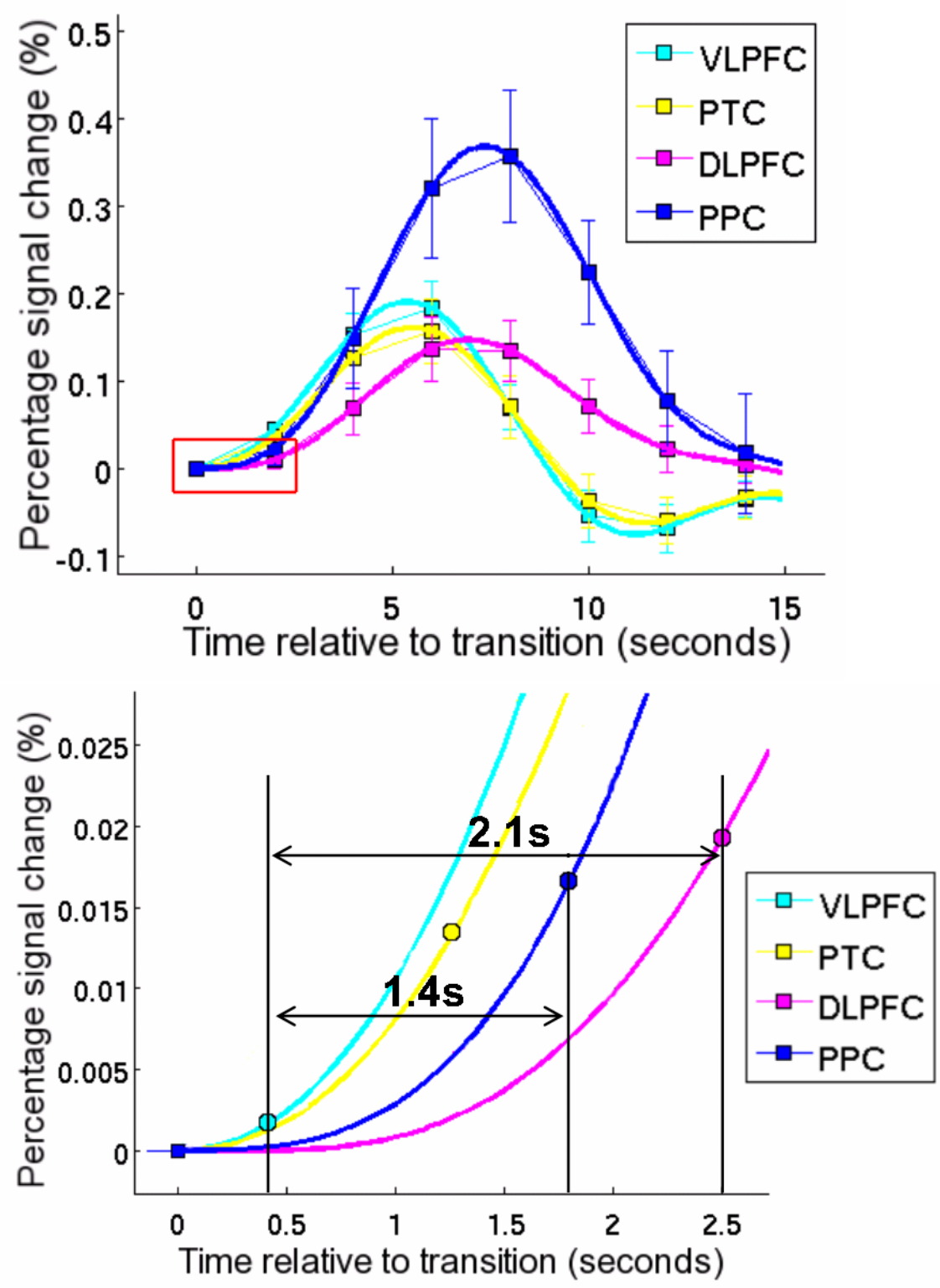

(Top panel) Fourier basis fitted-event responses. Event-related BOLD responses from the VLPFC (cyan), PTC (yellow), DLPFC (magenta) and PPC (blue) were fitted with a sixth order Fourier basis set (windowed with a Hanning function) and averaged across subjects. Error bars show s.e.m. across subjects; error bars are shown at each TR for demonstration purposes. Thin lines of the same color connect successive values of the fitted response at each TR.

(Bottom panel) Magnified view of red box in top panel (error bars have been removed for clarity). Onset latencies were defined as the time at which the slope of the fitted response exceeded 10% of the maximum slope of the ascending part of the response. Colored circles indicate onset times of the different regions (same color scheme as previous panel). Onset of BOLD response for the VLPFC (cyan) led the onset of the DLPFC (magenta) by 2.1s ($p<0.05$, Wilcoxon signed rank test) and the PPC (blue) by 1.4s ($p<0.01$, Wilcoxon signed rank test). The mean onset latency of the PTC (yellow) also led the DLPFC and PPC, although pair-wise differences in onset were not significant (see also Figure 5B in main text).

Figure S2. Brain regions that track fluctuations in the amplitude envelope.

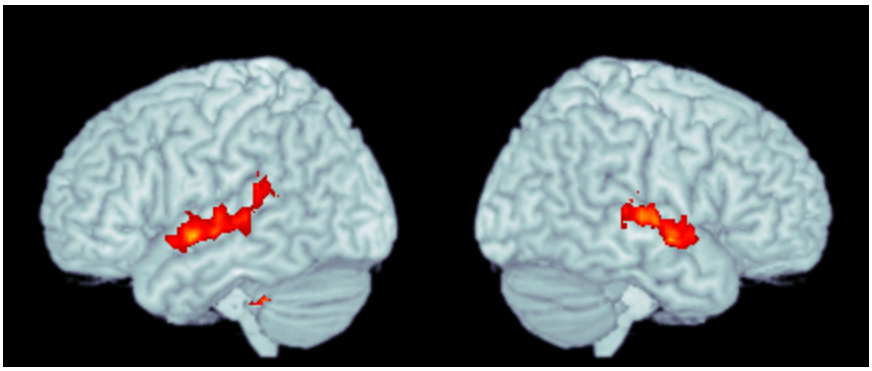

General linear model (GLM) analysis with amplitude envelope as the variable of interest revealed activation of only the bilateral auditory cortices along the dorsal part of the superior temporal gyrus. Thus, amplitude variation in the stimulus cannot, by itself, explain the pattern of activation observed during the transition.

Figure S3. Comparison of brain responses to movement transitions versus auditory oddball stimuli.

Oddball Task

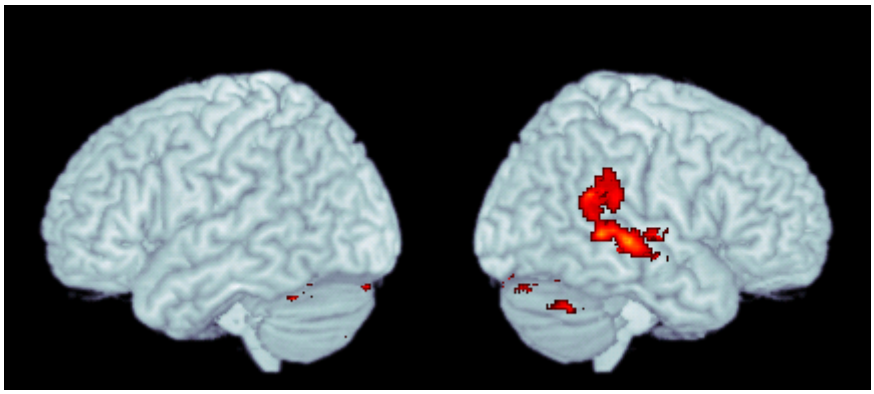

Movement Transition

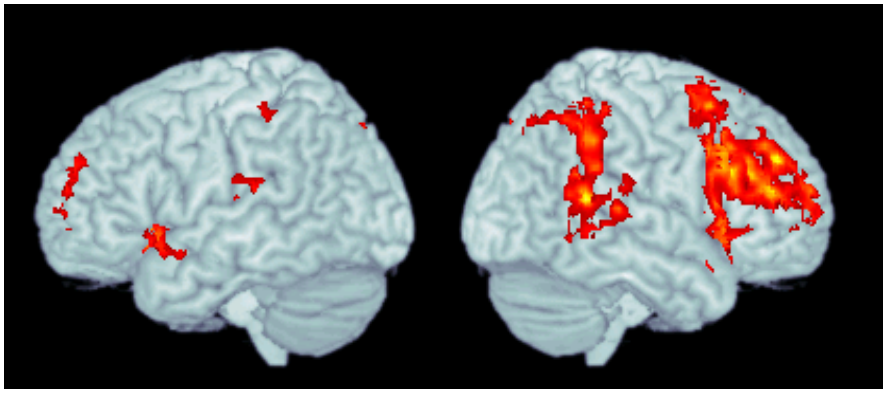

Transitions – Oddball

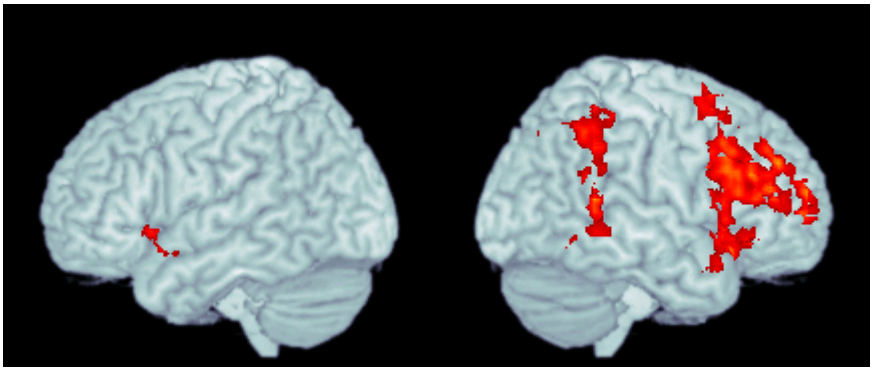

(Top panel) Activations to infrequent, compared to frequent, stimuli during an auditory oddball task (Crottaz-Herbette and Menon, 2006).

(Middle panel) Activations observed during movement transitions (reproduced from Fig 2A; t= 0s).

(Bottom panel) A between-task analysis was conducted to identify brain areas that showed greater activation during the movement transition compared to the auditory oddball task.

Both qualitative and quantitative differences were observed between the tasks. Activations in the PTC, cingulate cortex and cerebellum overlapped with activations observed in the present study (see also Table S3). However, the PTC and extended regions of the TPJ showed greater activation during movement transitions. Other areas such as the VLPFC, PPC and DLPFC, which showed strong activation during the movement transition, did not show statistically significant activation during the auditory oddball task. Thus, the oddball task does not recruit the extensive dorsal and ventral network activations observed during passive segmentation in the present study. Further, the between-task comparison (bottom panel) revealed almost exactly the same set of regions that were active during the transition (middle panel; also see Table S4 and compare with Table S2), indicating significant quantitative differences between the oddball task activations and the dorsal-ventral stream activations observed in the present study. These findings indicate that brain processes engaged during the perception of the movement transition are distinct from those elicited by the oddball task.

Figure S4. RR-variability in a 10-second time window surrounding the movement transition.

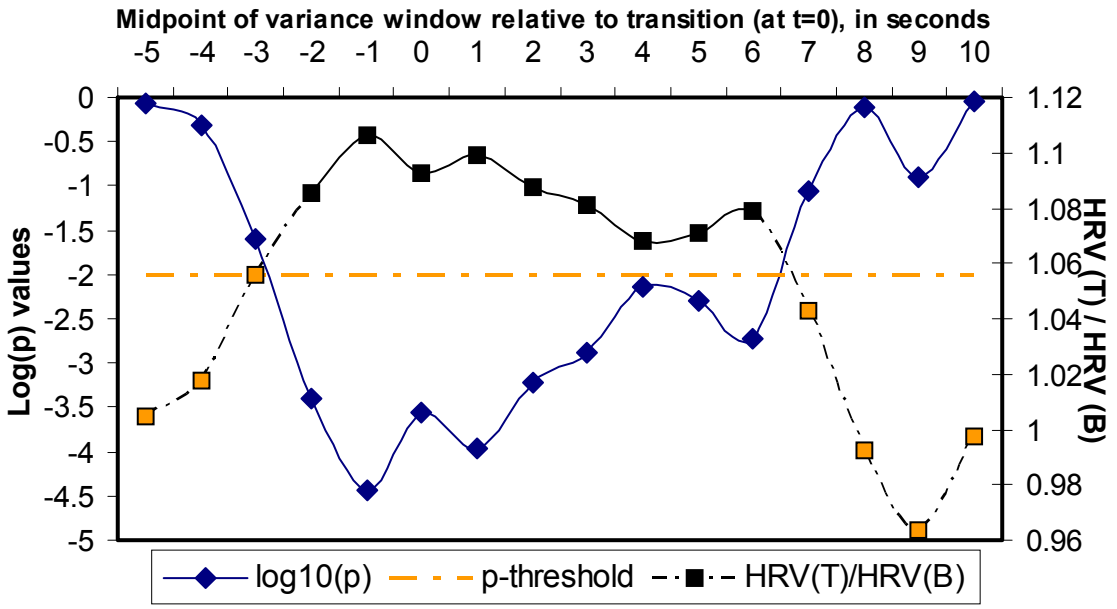

R-R variability was significantly higher during the movement transition. Logarithm of p values for the F-test for significant difference of HRV between observation window and baseline plotted (dark blue diamonds) against the midpoint of the moving observation window. Observation window size was fixed at 10s; the observation window was translated in time such that its midpoint went from t= -5s to t=+10s (t=0s represents the point of transition). The F-test returned significant results chiefly for observation windows that encompassed the transition. P-threshold (0.01) is shown as dash-dotted red line. On the right hand side Y-axis, the ratio of the HRV during the transition to that during the baseline (black and orange squares) is plotted. HRV within the transition window was higher than baseline HRV. Windows centered up to 6s after the point of transition show a significantly higher HRV, indicative of the physiological response lag. Ratios plotted as orange squares correspond to non-significant p-values for the F-test. Intermediate values are spline interpolated for demonstration purposes only.

Figure S5. Validation of the mental chronometric method of Sterzer and Kleinschmidt (2007) used in the main text.

Figure S5-A. Converging evidence with alternate method for calculating onset latencies (Menon et al., 1998).

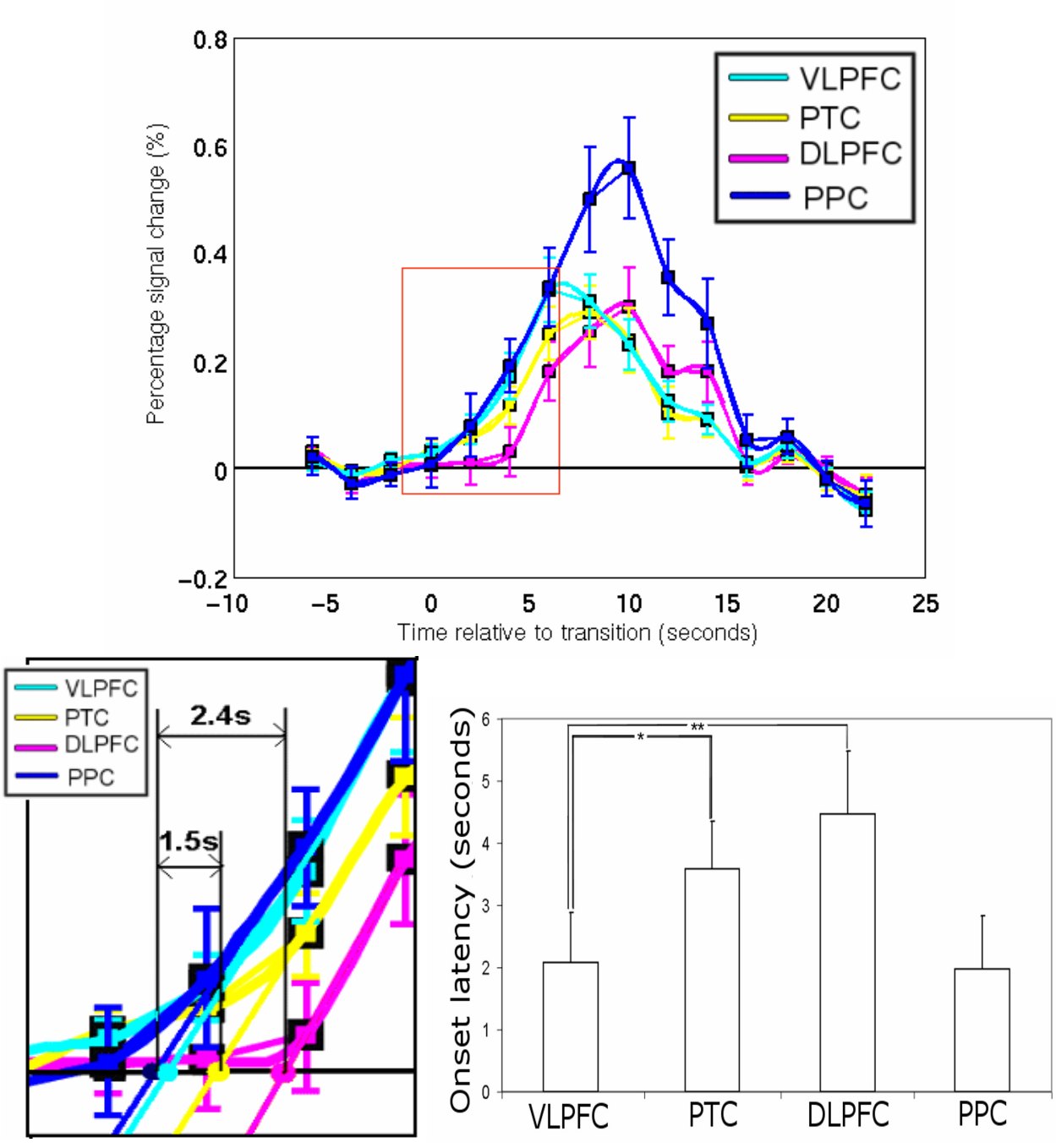

(Top panel) Raw event-related BOLD responses from the VLPFC (cyan), PTC (yellow), DLPFC (magenta) and PPC (blue) averaged across subjects. The BOLD response is spline interpolated (thick curve) for demonstration purposes. Thin lines of the same color connecting successive points in the BOLD response are also shown for reference (error bars show s.e.m. across subjects). The percentage signal change for the raw response appears to have a higher magnitude then the fitted response (Figure S1) due to the different ways baselines were assessed in each case; however, this does not affect our results, as the onset latency computation depends only on the relative slopes and not on the magnitudes of the percentage change in signal (as we are interested only in the difference in onset latencies, and not their absolute values).

(Bottom panel, left) Onset latencies are calculated by fitting a line to linear portion of the BOLD response of the right hemispheric ROIs (red box in top panel) and extrapolating this line to the x-axis (colored circles denote onset latiencies, i.e. point of intersection of the fitted line with the x-axis, of the respective ROIs). The DLPFC (magenta) lags the VLPFC(cyan) by 2.4s ($p<0.01$) and the PTC (yellow) lags the VLPFC by 1.5s ($p<0.05$).

(Bottom panel, right) The mean and standard error of onset latencies across subjects. These results show that the VLPFC has the earliest onset among all ROIs and leads the DLPFC by more than two seconds ($p<0.01$), providing convergence with the results obtained from the method of Sterzer and Kleinschmidt (2007) used in the main text.

Figure S5-B. Converging evidence with another dataset (Steinberg working memory task, Chang et al., 2007).

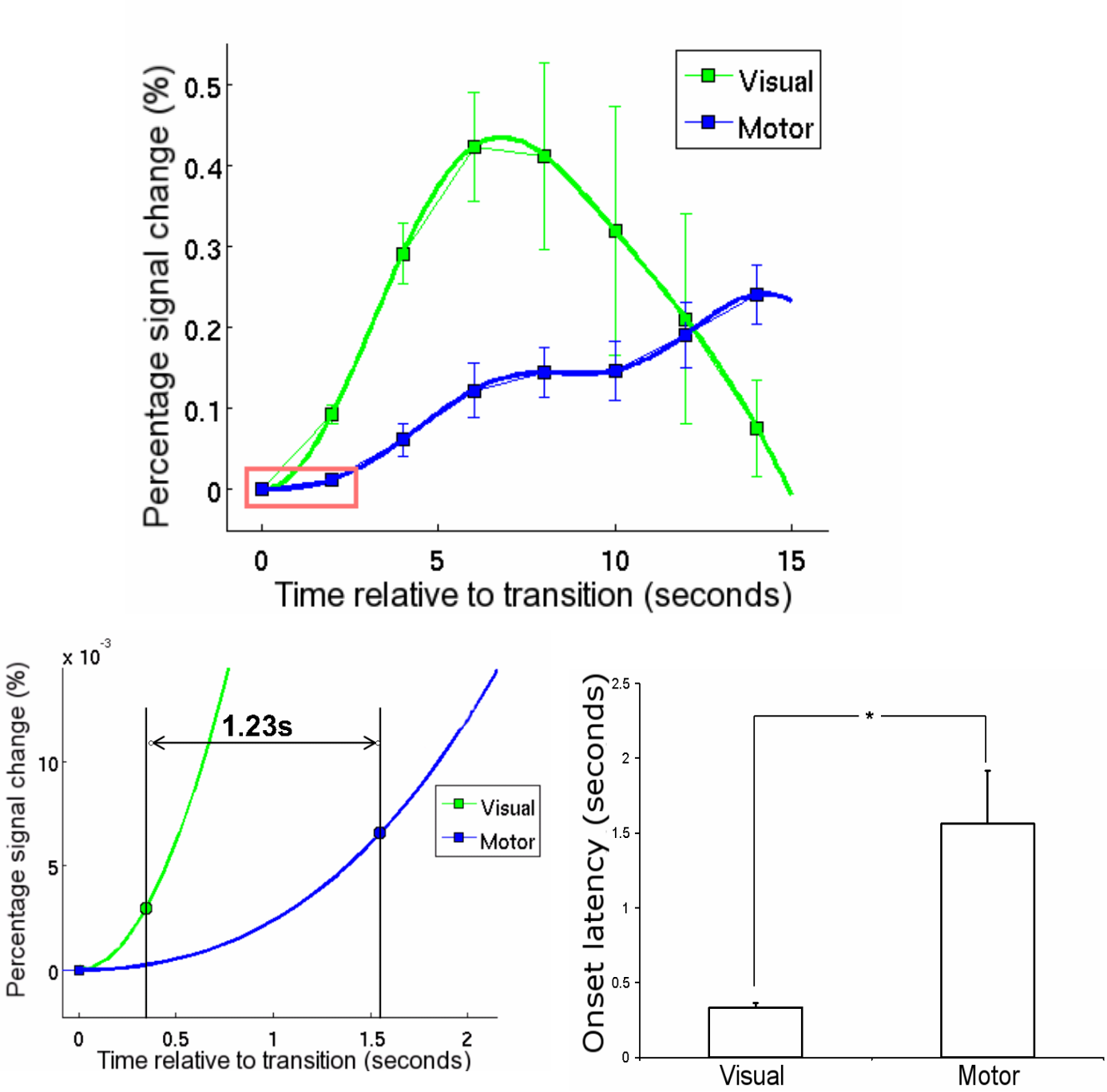

(Top panel) Fourier basis fitted event responses for the Stienberg working memory dataset (Chang et al., 2007). Event-related BOLD responses from the visual cortex (left hemispheric

inferior occipital gyrus, green) and motor cortex (precentral gyrus, blue) were fitted with a sixth-order Fourier basis set (windowed with a Hanning function) and averaged across subjects (as in Figure S1). Error bars show s.e.m. across subjects; error bars are shown at each TR for demonstration purposes. Thin lines of the same color connect successive values of the fitted response at each TR.

(Bottom panel, left) Magnified view of red box in top panel (error bars have been removed for clarity). Onset latencies were defined as in Figure S1. Colored circles indicate onset times of the different regions (same color scheme as previous panel). Onset of BOLD response for the visual cortex led the onset of the motor cortex by 1.23s ($p=0.0103$, Wilcoxon signed rank test).

(Bottom panel, right) The mean and standard error of onset latencies across subjects. Onset latencies, quantified across subjects, show that the visual cortex onsets earlier than the motor cortex. This was indeed as expected because the Steinberg task required a visual response of the subject in the encoding phase before a motor response could occur in the response phase.

Figure S6. Validation of the Granger causal analysis technique (Roebroeck et al., 2005) used in the main text.

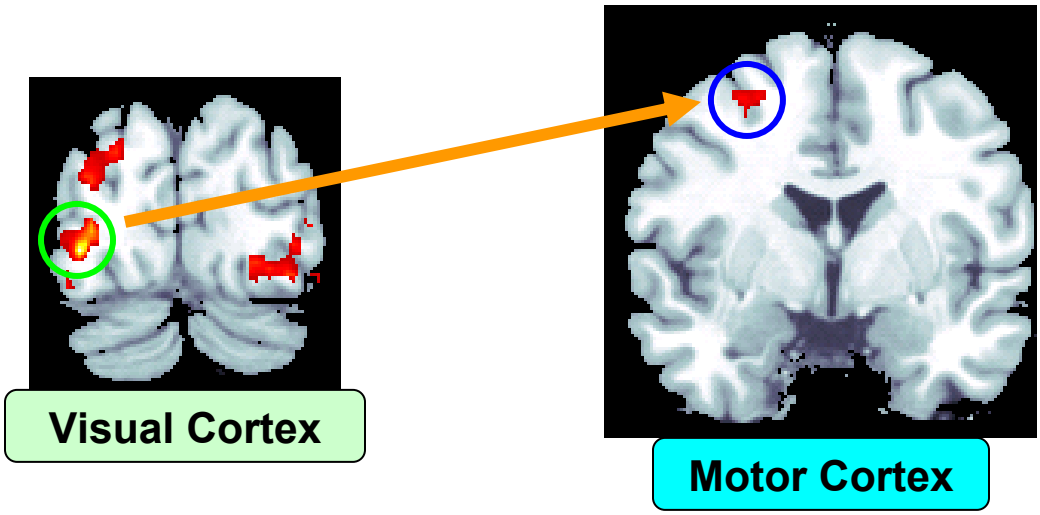

Granger causal analysis of the visual (left inferior occipital cortex [y=-86mm], circled in green, left panel) and motor (precentral gyrus [y=-1mm], circled in blue, right panel) regions from the Steinberg dataset showed a causal link from the visual cortex to the motor cortex, in conformity with the pattern of observed onset latency differences. These control analyses (Figure S5 and Figure S6) further increase confidence in our methods of chronometric (onset latency) analysis and Granger causality analysis.

Table S1. Individual participant responses to potential movement transitions in the stimuli.

Subject No.	N_l	N_a	N_w	T_l	T_a	T_w
1	12	18	12	0.60	0.90	1.00
2	15	20	16	0.75	1.00	0.94
3	15	19	20	0.75	0.95	0.75
4	10	13	16	0.50	0.65	0.63
5	17	24	20	0.85	1.20	0.85
6	17	20	21	0.85	1.00	0.81
7	19	20	22	0.95	1.00	0.86
8	9	9	16	0.45	0.45	0.56
9	16	18	20	0.80	0.90	0.80
10	18	20	31	0.90	1.00	0.58
Mean	14.8	18.1	19.4	**0.74**	**0.91**	**0.78**

N_l = Number of large transitions indicated within observation window (see text for details)

N_a = Number of large and small transitions indicated within the observation window

N_w = Total number of large transitions indicated by the subjects (both within and outside the observation window)

N_m = Actual number of movement transitions in the stimulus = 20.

$T_l = N_l / N_m$; $T_a = N_a / N_m$; $T_w = N_l / N_w$ (see text for details)

Table S2. Brain activations elicited by the movement transition.

Regions	BA	P-value (corr.)	# of Voxels	Max. Z-Score	Peak-MNI coords (mm)
R VLPFC, Insula, and Temporal pole	47, 44/45, 38	0.000	726	4.92	30 24 -8
R DLPFC	9/46	0.000	5646	5.26	38 46 30
R PPC and R Middle temporal gyrus (PTC)	40, 21/22	0.000	2459	5.15	64 -46 12
Anterior & Mid-cingulate cortex	24/32	0.000	2250	5.07	4 34 44
L superior temporal gyrus	22	0.001	368	5.36	-46 -26 6
L and R Caudate and Thalamus	--	0.000	1530	4.30	10 -12 8
L and R Precuneus	--	0.000	951	4.92	0 -48 44
L Cerebellum	--	0.002	337	4.09	-16 -80 -36

Abbreviations:

L: left; R: right

DLPFC: Dorsolateral prefrontal cortex

PPC: Posterior parietal cortex

PTC: Posterior temporal cortex

VLPFC: Ventrolateral prefrontal cortex

Table S3. Brain activations elicited during an auditory oddball task to infrequent vs. frequent stimuli.

Regions	BA	P-value (corr.)	# of Voxels	Max. Z-Score	Peak-MNI coords (mm)
R Middle temporal gyrus	21/22	0.000	866	4.21	54 -36 2
Mid-cingulate cortex	32	0.010	396	3.96	4 16 44
Bilateral thalamus (dorsomedial)	-	0.040	311	3.67	8 -20 12
R Cerebellum	-	0.012	384	3.53	32 -68 -26
Bilateral cerebellar vermis	-	0.000	1088	4.36	4 -84 -18

Abbreviations:

L: left; R: right

Table S4. Brain areas that showed greater activation during the movement transition compared to the auditory oddball task.

Regions	BA	P-value (corr.)	# of Voxels	Max. Z-Score	Peak-MNI coords (mm)
R VLPFC, Insula, and Temporal pole	47, 44/45, 38	0.000	493	4.77	30 24 -6
R DLPFC	9/46	0.000	4278	5.15	38 46 30
R PPC and R Middle temporal gyrus (PTC)	40, 21/22	0.034	230	4.70	64 -46 12
Anterior & Mid-cingulate cortex	24/32	0.000	1193	4.84	0 30 42
R PPC	40/39	0.000	754	3.84	50 -50 46

Abbreviations:

L: left; R: right

DLPFC: Dorsolateral prefrontal cortex

PPC: Posterior parietal cortex

PTC: Posterior temporal cortex

VLPFC: Ventrolateral prefrontal cortex